

**Bifurcations in models of a society of reasonable contrarians and conformists**

Franco Bagnoli\*

*Dipartimento di Fisica e Astronomia, Università di Firenze, Via G. Sansone 1, 50017 Sesto Fiorentino, Firenze, Italy  
and INFN, Sezione di Firenze, Firenze, Italy*

Raúl Rechtman†

*Instituto de Energías Renovables, Universidad Nacional Autónoma de México, Apartado Postal 34, 62580 Temixco, Morelos, Mexico*

(Received 4 March 2015; revised manuscript received 11 July 2015; published 14 October 2015)

We study models of a society composed of a mixture of conformist and reasonable contrarian agents that at any instant hold one of two opinions. Conformists tend to agree with the average opinion of their neighbors and reasonable contrarians tend to disagree, but revert to a conformist behavior in the presence of an overwhelming majority, in line with psychological experiments. The model is studied in the mean-field approximation and on small-world and scale-free networks. In the mean-field approximation, a large fraction of conformists triggers a polarization of the opinions, a pitchfork bifurcation, while a majority of reasonable contrarians leads to coherent oscillations, with an alternation of period-doubling and pitchfork bifurcations up to chaos. Similar scenarios are obtained by changing the fraction of long-range rewiring and the parameter of scale-free networks related to the average connectivity.

DOI: [10.1103/PhysRevE.92.042913](https://doi.org/10.1103/PhysRevE.92.042913)

PACS number(s): 05.45.Ac, 05.50.+q, 64.60.aq, 64.60.Ht

**I. INTRODUCTION**

The study of social dynamics and opinion formation in a society is an interesting topic in statistical physics [1–3]. We study a society whose agents have one of two opinions that change synchronously in time. Opinion formation models where agents have a continuous opinion have also been studied extensively [1,4–6]. It is common to classify the attitude of people (agents) as either conformist or contrarian (also known as nonconformist). A conformist tends to agree with his neighbors and a contrarian to disagree. Clearly, this is a crude approximation of society, but the one we follow below.

Models where agents can express one of two opinions are in many cases extensions of the Ising model where the collective opinion is the equivalent of magnetization. The site variable represents an agent's opinion and the coupling of a conformist agent with neighbors is ferromagnetic and that of a contrarian agent is antiferromagnetic [1,7]. The simple ferromagnetic Ising model represents a uniform society of conformists with local interactions. Many aspects of this model may be varied: the interaction network, which in societies is quite different from a regular lattice; the uniformity of the society; and the response to the others' influence.

Contrarians were introduced in a different sociophysical model by Galam [8,9]. In this case they had the effect of destroying consensus in a society mainly formed by conformists. When the fraction of contrarians becomes opinion dependent, chaotic dynamics is present [10]. The presence of contrarian agents in a society has been studied in models related to the voter model [11–15].

One of most intriguing effects is the hipster's, in which a society of contrarians tends to behave in a uniform way due to a sort of synchronization effect [16]. Clearly, conformist

hipsters always change their behavior when they realize they are still in the mainstream. This effect is due to a sort of synchronization among people and we show that, paradoxically, this synchronization can be promoted by a fraction of conformists.

Individuals that are under strong social pressure tend to agree with the great majority even when they are certain that the majority's opinion is wrong, as shown by Asch [17]. An agent can be either a conformist who agrees with one's neighbors or a contrarian who disagrees: a linear interaction. Under strong social pressure a contrarian may agree with a large majority: a nonlinear interaction. Following an overwhelming majority is an ecological strategy since it is probable that this coherent behavior is due to some unknown piece of information and in any case the competitive loss is minimal since it equally affects the other agents.

In a previous work [7] we referred to this nonlinear contrarian attitude as a reasonable contrarian. There we studied the collective behavior of a uniform society of reasonable contrarian agents. The rationale was that in some cases, in particular in the presence of frustrated situations such as in minority games [18], it is inconvenient to always follow the majority since in this case one is always on the losing side of the market. This is one of the main reasons for the emergence of a contrarian attitude. On the other hand, if all or almost all agents in a market make the same decision, it is often wise to follow such a trend. We call such a situation the social norm. A society fully composed of reasonable contrarians exhibits interesting behaviors when changing the topology of the connections. On a one-dimensional regular lattice, there is no long-range order, the evolution is disordered, and the average opinion is always halfway between the extreme values 0 and 1. However, adding long-range connections or rewiring existing ones, we observe the Watts-Strogatz small-world effect, with a transition towards a mean-field behavior. However, since in this case the mean-field equation is, for a suitable choice of parameters, chaotic, we observe the emergence of coherent

\*franco.bagnoli@unifi.it

†rrs@ier.unam.mx

oscillations, with a bifurcation cascade eventually leading to a chaoticlike behavior of the average opinion. The small-world transition is essentially a synchronization effect. Similar effects with a bifurcation diagram resembling that of the logistic map have been observed in a different model of adapt if novel and drop if ubiquitous behavior, upon changing the connectivity [19,20].

Since a homogeneous society of unreasonable contrarians is not so reasonable, we study here the collective behavior of a society composed of a mixture of conformists and contrarians. To keep things simple, reasonable contrarian and conformist agents have the same behavior in the presence of an overwhelming majority of their neighbors. Conformists become less conformist in the presence of a large majority. We can call them slightly unreasonable. The presence of reasonable contrarians and slightly unreasonable contrarians avoids absorbing states, which are rather unusual in real societies.

In the presence of a strong fraction of conformists, we have the classical ferromagnetic Ising scenario, with the appearance of a stationary average opinion different from one-half. As this fraction becomes smaller, this polarized opinion vanishes, as expected. What is unexpected is the appearance of another bifurcation, with oscillations and the transition to chaos or disorder as the fraction of conformists becomes smaller.

The outline of the present paper is as follows. In Sec. II we present the model in detail. Its mean-field approximation is discussed in Sec. III. Then the model is studied on small-world networks in Sec. IV and on scale-free networks in Sec. V. A summary is given in Sec. VI.

## II. MODEL

Our model society is formed by  $N$  agents with a fraction  $\xi$  of conformists and a fraction  $1 - \xi$  of contrarians. Agent  $i$ ,  $i = 0, \dots, N - 1$ , holds an opinion  $s(i, t) \in \{0, 1\}$  at time  $t$ . The opinions of all agents change synchronously in time. Agent  $i$  gathers the average opinion of neighbors and changes one's opinion, tending to agree with neighbors if one is a conformist or to disagree if one is a contrarian.

The neighborhoods of all agents are defined by the adjacency matrix  $A$  with components  $a_{ij} \in \{0, 1\}$  in a way such that  $a_{ij} = 1$  if agent  $j$  belongs to  $i$ 's neighborhood and  $a_{ij} = 0$  if one does not. The connectivity  $k_i$  of agent  $i$  given by neighborhood

$$k_i = \sum_j a_{ij} \quad (1)$$

is the number of agents in  $i$ 's neighborhood and the average opinion  $h_i$  of  $i$ 's neighbors is

$$h_i = \frac{1}{k_i} \sum_j a_{ij} s(j). \quad (2)$$

The average opinion  $c$  of the society is

$$c = \frac{1}{N} \sum_i s_i. \quad (3)$$

Given the average opinion  $h$  of the neighbors of agent  $i$  at time  $t$ ,  $s(i, t + 1) = 1$  according to the transition probability

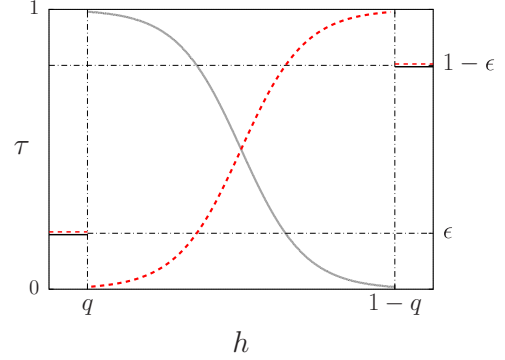


FIG. 1. (Color online) Transition probabilities  $\tau$  given by Eq. (4). For  $q < h < 1 - q$ ,  $\tau$  is an increasing function of  $h$  (red dashed curve) for conformists, with  $J = 3$ , and a decreasing one (black solid curve) for reasonable contrarians, with  $J = -3$ . In this and the following figures  $q = 0.1$  and  $\varepsilon = 0.2$  unless stated otherwise.

$\tau(h; J)$  defined by [7]

$$\tau(h; J) = \begin{cases} \varepsilon & \text{for } h < q \\ \frac{1}{1 + \exp[-2J(2h-1)]} & \text{for } q \leq h \leq 1 - q \\ 1 - \varepsilon & \text{for } h > 1 - q. \end{cases} \quad (4)$$

In this expression  $J$  represents the agent's conviction: Conformists have  $J > 0$  and reasonable contrarians  $J < 0$ . The graphs of  $\tau$  are shown in Fig. 1. When the average opinion  $h$  is smaller than  $q$  or larger than  $1 - q$  a reasonable contrarian agent will likely agree with neighbors and the likeliness depends on the factor  $\varepsilon$ . Since  $\varepsilon$  is small an agent will probably agree with the majority when  $0 < q < h$  or  $1 - q < h < 1$  whether the agent is a contrarian or a conformist. This is a way of implementing the effect of social norms. The fact that  $\varepsilon > 0$  also avoids the presence of absorbing states but causes the slightly unreasonable behavior of conformists.

In the intermediate case  $q < h < 1 - q$ , a conformist ( $J > 0$ ) will probably agree with neighbors and a reasonable contrarian ( $J < 0$ ) will probably disagree. Both conformists and contrarians share the same values of  $|J|$ ,  $q$ , and  $\varepsilon$ . Unless stated otherwise, we always use the values  $q = 0.1$  and  $\varepsilon = 0.2$ , as in Ref. [7]. A discussion about alternative choices of the transition function is delayed after the introduction of the mean-field approximation in the following section.

In the mean-field approximation  $c$  changes deterministically and the Lyapunov exponent  $\lambda$  is a good indicator of the stability of any orbit [21]. Boltzmann's entropy  $\eta$  of the probability distribution of  $c$  is another indicator of stability and can be computed both for deterministic and stochastic (extended) systems [7,22]. To compute  $\eta$ , we partition the unit interval in  $L$  disjoint equal-sized subintervals  $I_i$ ,  $i = 0, \dots, L - 1$ , and find  $q_i$  as the fraction of visits of a long time orbit of  $T$  time steps to  $I_i$ . Then

$$\eta = \frac{-1}{\log L} \sum_{i=1}^L q_i \log q_i. \quad (5)$$

In numerical simulations  $T \gg L$ . A fixed point of the trajectory corresponds to  $\eta = 0$  and when the orbit visits every subinterval  $I_i$  with the same frequency  $\eta = 1$ . If  $L = 2^b$  and

the orbit is periodic with period  $2^a$ ,  $\eta = a/b$ . In the limit  $L \rightarrow \infty$ ,  $\eta \rightarrow 0$  for periodic orbits.

For deterministic maps we can compare the behavior of the Lyapunov exponent  $\lambda$  and that of Boltzmann's entropy  $\eta$  [see Fig. 4(b)]. Values of  $\lambda > 0$  are equivalent to  $\eta > 1/2$  when  $L$  is sufficiently large. In other words, deterministic chaos corresponds to  $\eta > 1/2$  and order to  $\eta < 1/2$ . By extending this correspondence to the probabilistic network dynamics, we define disorder whenever  $\eta \gtrsim 1/2$  and order when  $\eta \lesssim 1/2$ .

### III. MEAN-FIELD APPROXIMATION

We start with a model of a society where the neighborhood of each agent  $i$ , either conformist or contrarian, is formed by  $k$  random neighbors, i.e., the mean-field approximation for a fixed connectivity  $k$ . With a fraction  $\xi$  of conformists and a fraction  $1 - \xi$  of reasonable contrarians, the time evolution of the average opinion  $c$  is

$$c' = \sum_{w=0}^k \binom{k}{w} c^w (1-c)^{k-w} \times [\xi \tau(w/k; J) + (1-\xi) \tau(w/k; -J)], \quad (6)$$

with  $c$  and  $c'$  the average opinions at times  $t$  and  $t + 1$ , respectively. In the right-hand side term, the term in large parentheses is the  $w$  combinations from a set of  $k$  elements.

In Fig. 2 we show return maps of Eq. (6) for different values of  $\xi$ . For small  $\xi$  [Fig. 2(a)] the map is chaotic and for larger values of  $\xi$  we find periodic orbits or fixed points [Figs. 2(b)–2(d)].

In Fig. 3 we show the mean-field bifurcation diagrams of  $c$  given by Eq. (6) as a function of the fraction of conformists  $\xi$  for  $\varepsilon = 0.2$  and  $\varepsilon = 0$ . In the second case, there are absorbing states for large  $\xi$ , but for smaller values the diagram hardly

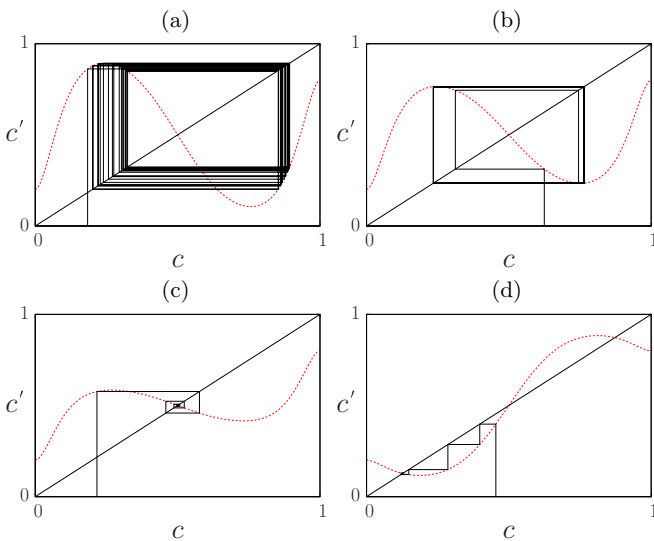


FIG. 2. (Color online) Return maps of the mean-field approximation (6) (red dashed curve) and 40 iterates of the map starting from a random initial  $c$  (black solid lines) for (a)  $\xi = 0.06$ , (b)  $\xi = 0.2$ , (c)  $\xi = 0.4$ , and (d)  $\xi = 0.9$ . In this and the following figures  $|J| = 5$  and  $k = 20$ .

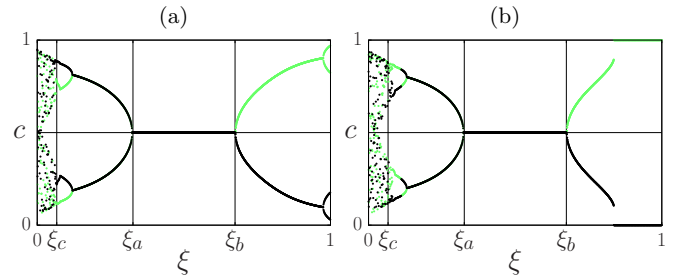


FIG. 3. (Color online) Mean-field average opinion  $c$  as a function of the fraction of conformists  $\xi$  for  $\xi_a = 0.3245$ ,  $\xi_b = 0.6755$ , and (a)  $\varepsilon = 0.2$  and  $\xi_c = 0.0665$  and (b)  $\varepsilon = 0.0$  and  $\xi_c = 0.0795$ . For  $\xi$  slightly larger than  $\xi_c$  the first and third branches starting from the bottom correspond to  $c_0 = 0.9$  [light gray (green)] and the other two to  $c_0 = 0.1$  (black). For  $\xi_b < \xi \leq 1$  the upper branch [light gray (green)] corresponds to  $c_0 = 0.9$  and the lower one (black) to  $c_0 = 0.1$ . For all values of  $\xi$  two consecutive iterations are plotted after a transient of 1000 time steps for both values of  $c_0$ .

depends on the value of  $\varepsilon$ . The leftmost vertical line at  $\xi_c$  marks the threshold at which the chaotic region ends.

We are now ready to illustrate the rationale of our choice of the transition probability  $\tau$  and of the parameters  $q$  and  $\varepsilon$ . The fundamental motivation of our investigation is the exploration of the consequences of social norms, which represent a typical human behavior but are rarely investigated in the literature. There are many papers that examine the consequences of the ferromagnetic (conformism) or antiferromagnetic (contrarian) Fermi function  $\tau(H; J) = 1/\{1 + \exp[-2J(2h - 1)]\}$ . In order to model the reasonable contrarian effect, in Ref. [7] we chose to modify this function only at the extremes, inserting a threshold  $q$  for the transition from conformist to contrarian behavior. We then inserted the parameter  $\varepsilon$  in order to avoid the presence of absorbing states. The exact values of the parameters  $q$  and  $\varepsilon$  are not crucial, nor is the fact that  $\tau$  is

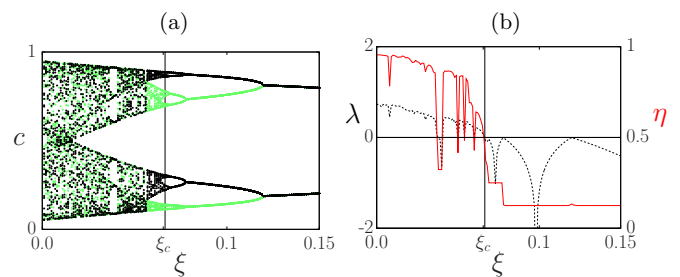


FIG. 4. (Color online) (a) Bifurcation diagram of the mean-field average opinion  $c$  as a function of the fraction of conformists  $\xi$  near  $\xi_c$ . For  $\xi$  slightly smaller and also larger than  $\xi_c$ , the first and third branches, starting from the bottom, correspond to  $c_0 = 0.9$  [light gray (green)] and the second and fourth to  $c_0 = 0.1$  (black). After a transient of 1000 time steps, 32 consecutive iterations are plotted for each value of  $\xi$  starting with  $c_0 = 0.9$  and  $0.1$ . (b) Lyapunov exponent  $\lambda$  (bottom black dashed curve for small  $\xi$ ) and the entropy  $\eta$  [top gray (red) solid curve for small  $\xi$ ] of the mean-field average opinion  $c$  [Eq. (6)] as functions of  $\xi$ . For each value of  $\xi$ ,  $\lambda$  is evaluated over 1000 time steps and for  $\eta$  the unit interval is divided in  $2^{10} = 1024$  equal-size subintervals and the probabilities  $q_i$  [Eq. (5)] are found over  $100 \times 2^{10} = 102\,400$  time steps after a transient of 300 time steps.

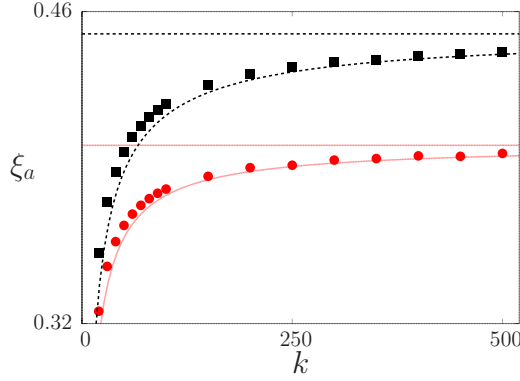


FIG. 5. (Color online) Mean-field critical values  $\xi_a$  as functions of  $k$  for  $|J| = 5$  [gray (red) circles] and  $|J| = 10$  (black squares). The solid curves are the graphs of Eq. (7): The bottom gray (red) solid curve is for  $|J| = 5$  and the top black dashed curve corresponds to  $|J| = 10$ . The horizontal lines show the asymptotic values (derived in the Appendix)  $\xi_a(5, \infty) = 0.4$  [bottom gray (red) solid line] and  $\xi_a(10, \infty) = 0.45$  (top black dashed line). Numerical data were obtained after a transient of 1000 time steps starting with  $c_0 = 0.9$ .

not continuous. We refer to the mean-field approximation to illustrate these points. The mean-field effect (6) is that of acting like a Gaussian smoothing convolution (see the Appendix), so the actual profile of the mean-field return map (Fig. 2) is smooth and rather insensitive to the details of the transition probability  $\tau$ . Since the width of the Gaussian-like mean-field smoothing depends on the quantity  $c(1-c)/k$ , these considerations hold for nonextreme values of the average opinion  $c$  and not extremely large sizes of the neighborhood. Indeed, one can see from Fig. 2 and the following phase diagrams that we are always interested in intermediate values of  $c$ . The only exception is Fig. 3, in which we report the influence of a change in the value of the parameter  $\varepsilon$ .

Actually, the role of the parameters  $q$  and  $\varepsilon$  can be played by a nonlinear term in the Fermi function, making  $\tau$  continuous. We anticipate that investigation of such a model will show that the modifications to the diagrams presented here are not essential for choices of the parameter  $W$  that make the mean-field curve similar to that obtained with the present values of  $q$  and  $\varepsilon$ . Since the goal of the present paper is to study the influence of a mixture of conformists and reasonable contrarians, we keep here the same form of  $\tau$  as in Ref. [7].

In Fig. 4(a) we show an enlargement of the bifurcation diagram for small  $\xi$  and in Fig. 4(b) the corresponding Lyapunov exponent  $\lambda$  and Boltzmann's entropy  $\eta$ . For  $\xi > \xi_c$ ,  $\lambda \leq 0$  and  $\eta \leq 1/2$ . In Figs. 3(a) and 3(b) [ $\xi_c, \xi_a$ ] corresponds to an inverse period-doubling bifurcation route from chaos to the fixed point  $c = 1/2$ . The rather large fraction of contrarians causes symmetric oscillations of  $c$ . The rightmost vertical line at  $\xi_b$  corresponds to a pitchfork bifurcation from  $c = 1/2$  to  $c > 1/2$  when  $c_0 > 1/2$  and to  $c < 1/2$  when  $c_0 < 1/2$  with  $c_0$  the average opinion at  $t = 0$  (see also Fig. 2).

We prove in the Appendix that  $\xi_a = 1 - \xi_b$  and find that the approximate behavior of  $\xi_a$  as a function of  $J$  and  $k$  is given by

$$\xi_a(J, k) = \frac{1}{2} \left( 1 - \frac{1}{J} \sqrt{1 + \frac{2J^2}{k}} \right). \quad (7)$$

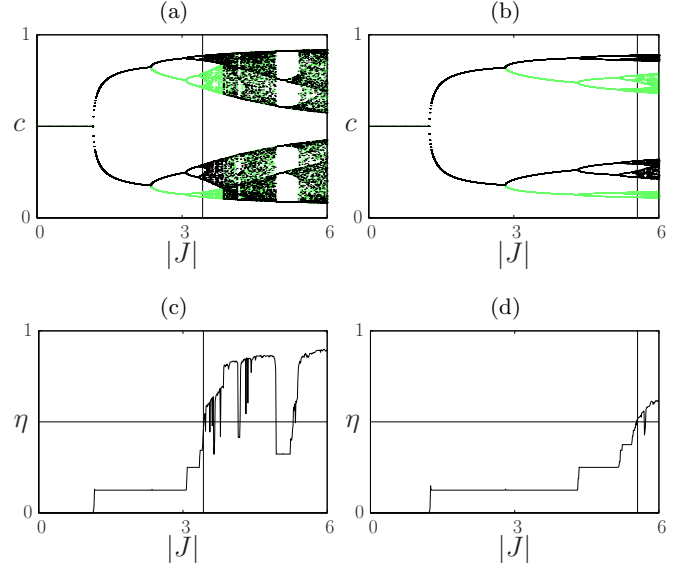


FIG. 6. (Color online) Mean-field bifurcation diagrams of the average opinion  $c$  and the corresponding entropies  $\eta$  as functions of  $|J|$  for (a)  $\xi = 0.04$  and (b)  $\xi = 0.07$ . Starting from small  $|J|$  there is a first bifurcation to a period-2 orbit, followed by a pitchfork bifurcation to four branches that correspond to period-2 orbits that depend on the initial value of  $c$ ,  $c_0$ . Starting from the bottom, the first and third branches correspond to  $c_0 = 0.9$  [light gray (green)] and the second and fourth to  $c_0 = 0.1$  (black). For larger values of  $|J|$  there are two period-doubling bifurcations cascading towards chaos. The vertical lines mark the transition to chaos obtained from the data shown in (c)  $|J| = 3.425$  and (d)  $|J| = 5.555$  as the smallest value of  $|J|$  for which  $\eta = 1/2$ . For each value of  $|J|$ , after a transient of 1000 time steps, the next 32 iterations are plotted for two initial average opinions  $c_0$ . (c) and (d) For the entropies, the unit interval is partitioned in  $L = 2^8 = 256$  subintervals. For each value of  $|J|$ , after a transient of 1000 time steps, the next 25 600 iterates are used to find the probabilities  $q_i$  and from them  $\eta$  [Eq. (4)].

In Fig. 5 we show that Eq. (7) agrees with the numerical results for large connectivities  $k$ .

In Fig. 6 we show the bifurcation diagrams of the average opinion  $c$  as  $|J|$  changes, for small values of  $\xi$ , and the corresponding entropies. For small  $|J|$  [Figs. 6(a) and 6(b)],  $c = 1/2$  and as this parameter grows, there is a first bifurcation to a period-2 orbit followed by two period-2 pitchfork bifurcations that depend on the initial opinion  $c_0$ . For still larger values of  $|J|$  there are two period-2-doubling cascades towards chaos. The transition to chaos is shown by the vertical lines found as the smallest values of  $J$  for which  $\eta = 1/2$  [Figs. 6(c) and 6(d)].

#### IV. SMALL-WORLD NETWORKS

Real societies are neither random nor regular. It is interesting to study what happens when the topology changes due, for instance, to advances in the transportation system or to politics favoring mixing, etc. We studied the effect of rewiring a fraction  $p$  of links in a regular one-dimensional society with connectivity  $k$ . This leads to the small-world networks first discussed by Watts and Strogatz [23]. As  $p$ , the long-range

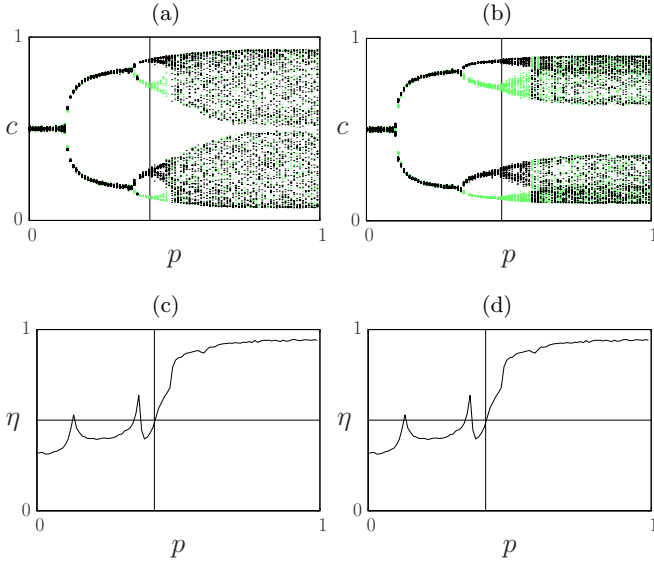


**FIG. 7.** (Color online) Small-world network bifurcation diagrams of the average opinion  $c$  and the corresponding entropies  $\eta$  as a function of the long-range connection probability  $p$  with  $N = 50\,000$ ,  $|J| = 5$ ,  $k = 20$ , and (a)  $\xi = 0.02$  and (b)  $\xi = 0.05$ . For  $p$  close to zero  $c$  oscillates around  $c = 0.5$  and as  $p$  grows there is a noisy period-2 bifurcation followed by two period-2 pitchfork bifurcations. Starting from the bottom, the first and third branches correspond to  $c_0 = 0.9$  [light gray (green)] and the second and fourth to  $c_0 = 0.2$  (black). The corresponding entropies are shown, where the value of  $p$  for which  $\eta = 0.5$  is shown as a vertical line (c)  $p = 0.415$  for  $\xi = 0.02$  and (d)  $p = 0.475$  for  $\xi = 0.05$ . For the bifurcation diagrams and for every value of  $p$ , the initial opinion of each agent is chosen at random between 0 and 1 with  $c_0 = 0.1$  [light gray (green) points] and  $c_0 = 0.9$  (black points). After a transient of 500 time steps, the next 64 values of  $c$  are plotted. For the entropies and for each value of  $p$  the unit interval is partitioned in  $L = 2^8 = 256$  subintervals. After a transient of 1000 time steps, the next 25 600 iterates are used to find the probabilities  $q_i$  and from them  $\eta$  [Eq. (5)].

connection probability, grows, small-world networks approach a mean-field behavior. As we show in Fig. 7, the bifurcation diagrams of  $c$  as functions of  $p$  are similar to those obtained by varying  $J$  in the mean-field approximation.

In Figs. 7(a) and 7(b) we show the bifurcation diagrams of  $c$  as functions of  $p$  for two small values of  $\xi$  and in Figs. 7(c) and 7(d) the corresponding entropies. For small  $p$ ,  $c$  fluctuates around  $c = 0.5$  and for slightly larger values, there are noisy oscillations around two symmetric values, in a way reminiscent of the period-doubling bifurcations of the mean-field approximation. For even larger values  $p \simeq 0.4$ , we observe the appearance of two different noisy period-2 oscillations that depend on the initial average opinion  $c_0$ . This roughly corresponds to what is shown in Fig. 6(a), although in that case the diagram is drawn as a function of  $|J|$  and here as a function of  $p$ .

For  $c = 0.2$  [Fig. 7(e)],  $c$  fluctuates around  $c = 0.5$  for small values of  $p$  and around two values for larger  $p$  that agree with the period-2 orbit of the mean-field approximation (6). For  $\xi = 0.8$  [Fig. 7(f)] and  $p \gtrsim 0.2$ ,  $c$  fluctuates around one of two values, depending on  $c_0$ , the average opinion at  $t = 0$ . These values also agree with the mean-field approximation.

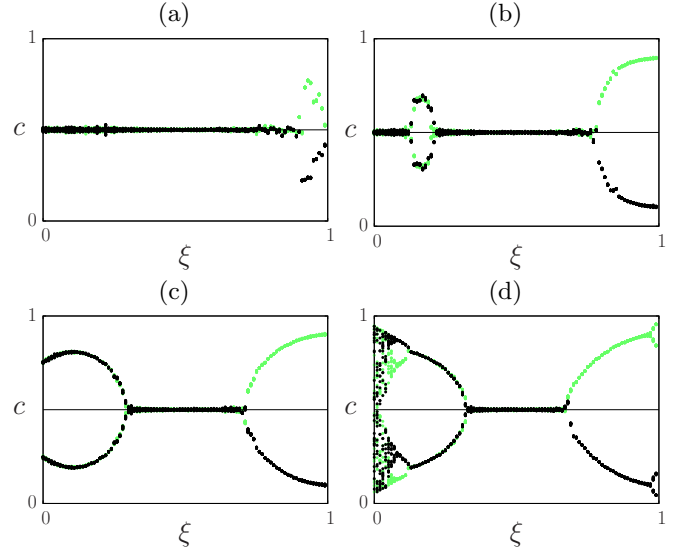


**FIG. 8.** (Color online) Small-world network bifurcation diagrams of the average opinion  $c$  and the corresponding entropies  $\eta$  as functions of the fraction of conformists  $\xi$  for different values of  $p$ : (a)  $p = 0.02$ , (b)  $p = 0.05$ , (c)  $p = 0.20$ , and (d)  $p = 0.80$ . For each value of  $\xi$ , at  $t = 0$ , the opinion of each agent is chosen at random in such a way that the average opinion is  $c_0 = 0.1$  or  $0.9$ . After a transient of 50 000 time steps, 64 points are plotted. For  $\xi$  near 1, the orbits that started with  $c_0 = 0.9$  have  $c > 1/2$  [light gray (green) points] and those that started with  $c_0 = 0.1$  have  $c < 1/2$  (black points). For smaller values of  $\xi$ , the points that correspond to  $c_0 = 0.1$  (black) almost mask those with  $C_0 = 0.9$ . In (d) there is a chaotic phase for small  $\xi$ .

It is possible to roughly understand these results assuming that the main contributions to the mean-field character of the collective behavior come from the fraction of links that are rewired (long-range connections) that depend on  $p$ . The actual value of the field  $2h - 1$  in Eq. (4) is multiplied by a factor  $p$ , so changing  $p$  is roughly equivalent to changing  $J$ .

In Fig. 8 we show bifurcation diagrams of  $c$  on small-world networks as a function of the fraction of conformists  $\xi$  for several values of the long-range connection probability  $p$ . This sequence of plots illustrates an unexpected behavior. For  $p = 0$  [Fig. 8(a)] there is a pitchfork bifurcation at  $\xi \sim 0.9$ . For larger values of  $p$  the pitchfork bifurcation occurs at smaller values of  $\xi$  and an oscillating bubble is formed [Fig. 8(b)] for  $0.12 \lesssim \xi \lesssim 0.22$ . This oscillating region grows with  $c$  and for  $p = 0.8$  [Fig. 8(d)] the bifurcation diagram is similar to the mean-field one [Fig. 3(a)].

We can explain this behavior by assuming that the conformist behavior promotes synchronization, as does  $p$ . So the system progressively synchronizes starting from high values of  $\xi$ , but this synchronization is not visible if the dynamics leads to fixed points. When the synchronization reaches the oscillating phases, it becomes manifest by means of the coherent oscillation of the population. So this coherent dynamical behavior appears to start first in the vicinity of the bifurcation for  $\xi \simeq 0.2$  and then, by increasing  $p$ , it propagates to lower values of  $\xi$ .

## V. SCALE-FREE NETWORKS

In this section we present results of the model on uncorrelated scale-free networks [24]. Starting from a fully connected group of  $m$  agents, other  $N - m$  agents join sequentially, each one choosing  $m$  neighbors among those already in the group. The following choice is preferred: The probability that a new member chooses agent  $i$  is proportional to its connectivity  $k_i$ , the number of neighboring agents that agent  $i$  already has. Another way of building the network is choosing a random edge of a random node and connecting to the other end of the edge, since such an edge arrives at a vertex with probability proportional to  $k p(k)$  with  $p(k)$  the probability that a randomly selected node has connectivity  $k$  [25].

In Ref. [7] we showed that the dynamics of a model of a society whose agents are all reasonable contrarians on a scale-free network with  $m$  initially connected agents is comparable to the mean-field approximation of Sec. III with connectivity  $k$  provided that

$$k = \alpha m \quad (8)$$

with  $\alpha \sim 1.7$  for scale-free networks with  $p(k) \propto k^{-3}$ . In Fig. 9 we show that this result also holds for the model of societies studied here. We compare the bifurcation diagrams (for  $\xi$  changing) of the dynamics on a scale-free network

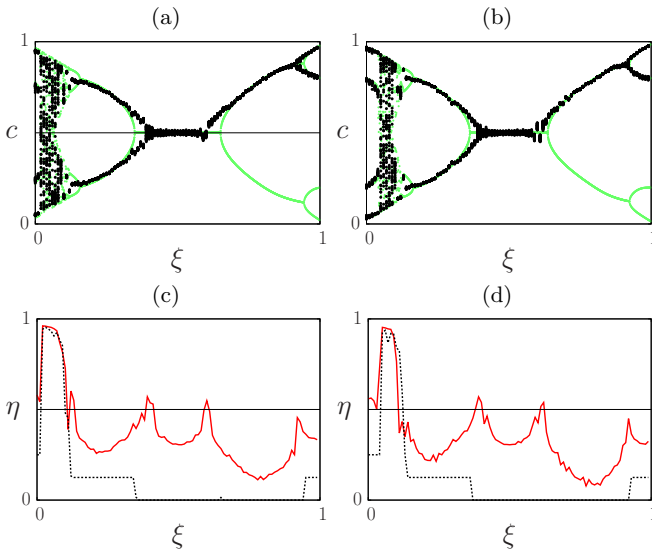


FIG. 9. (Color online) (a) and (b) Bifurcation diagrams of the average opinion  $c$  on a scale-free network (black large points) and the mean-field approximation (6) [light gray (green) smaller points] as functions of the fraction of conformists  $\xi$  for (a)  $m = 20$  and  $k = 1.7 \times 20 = 34$  and (b)  $m = 30$  and  $k = 1.7 \times 30 = 51$ . (c) and (d) Boltzmann entropies  $\eta$  on a scale-free network (top red solid curve) and the mean-field approximation (6) (bottom black dashed curve) for (c)  $m = 20$  and  $k = 34$  and (d)  $m = 30$  and  $k = 51$ . (a) and (b) For the scale-free network and for each value of  $\xi$ , the average opinion at  $t = 0$  is  $c_0 = 0.9$  and for the mean-field bifurcation diagram  $c_0 = 0.9$  and  $0.1$ . After a transient of 300 time steps, the next 32 values of  $c$  are plotted. For the entropies and each value of  $\xi$ , the unit interval is divided in  $2^8 = 256$  equal-size subintervals. After a transient of 300 time steps, the next  $100 \times 2^8 = 25\,600$  iterates are used to find the probabilities  $q_i$  and from them  $\eta$  [Eq. (4)].

with the corresponding mean-field one [Figs. 9(a) and 9(b)] and the scale-free entropies with those of the mean-field map [Figs. 9(c) and 9(d)]. There is reasonable agreement in both bifurcation diagrams. Both entropies show good agreement where there is disorder, that is,  $\eta > 1/2$ , but not when  $\eta < 1/2$ . This can be understood from the bifurcation diagrams. While the scale-free network dynamics is stochastic and therefore the orbit visits many subintervals, the mean-field one visits a smaller number. For example, for  $\xi = 0.2$ , the mean-field dynamics has period 2, so  $\eta = 2/8$  in both Figs. 9(c) and 9(d).

## VI. CONCLUSION

The dynamics of the mean-field approximation of the average opinion  $c$  [Eq. (6)] as a function of  $\xi$  is chaotic with periodic windows when  $0 < \xi < \xi_c$  and oscillates periodically between two symmetric values when  $\xi_c < \xi < \xi_a$ . For  $\xi_a < \xi < \xi_b$ ,  $c = 1/2$ , and for  $\xi_b < \xi$ ,  $c > 1/2$  ( $c < 1/2$ ) if  $c_0 = 0.9$  ( $c_0 = 0.1$ ). Also  $\xi_a \sim 1 - \xi_b$  and  $\xi_a$  approaches a limit value as  $k$  grows. Equation (6) depends on the connectivity  $k$  and on the transition probability  $\tau$ , which in turn depends on  $k$ ,  $|J|$ ,  $\varepsilon$ , and  $q$ . As far as we have explored the parameter space, the above description is generic, with the exception that for large values of  $k$  the chaotic phase is bounded below by  $\xi_d$ . For  $0 < \xi < \xi_d$  there are two period-2 orbits that depend on  $c_0$  and for  $\xi_d < \xi < \xi_c$  the orbits are chaotic with periodic windows.

The dynamics on small-world networks approaches that of the mean-field approximation as the long-range connection probability  $p$  grows. The dynamics of  $c$  on scale-free networks is similar to that of the mean-field approximation provided  $k = \alpha m$  with  $\alpha \sim 1.7$ .

In small-world networks for small values of  $p$  [Fig. 8(b)], the coherent oscillations appear first for a population with a small fraction of conformists rather than for a pure contrarian one. This is probably due to the fact that coherent oscillations are a signal of synchronization and the presence of conformists increases the synchronization. On the other hand, if the synchronized dynamics leads to a stable fixed point, the degree of synchronization is not manifest. As a result, the first synchronized zone is near the bifurcation point  $\xi \simeq 0$ .

In social terms, the paradoxical effect is that a society of hipsters can exhibit coherent oscillations if all participants change their mind after realizing they are in the mainstream, despite their attitude [16]. This is a sort of synchronization effect and is clearly promoted by long-range interactions, like those mediated by the Internet. For purely local interactions, the uniform hipster effect is not visible at a global level since the groups are not synchronized. However, a small fraction of conformists can greatly enhance this synchronization, thus promoting the sudden change of trends seen in the alternative fashion world.

## ACKNOWLEDGMENTS

We thank S. Galam and K. D. Harris for having pointed out their interesting contributions about the effects induced by the presence of contrarians and of chaotic bifurcations upon rewiring. The comments of the referees are also acknowledged. Interesting discussions with Héctor D. Cortés González and Maximiliano Valdez González are acknowledged. This work

was partially supported by project PAPIIT-DGAPA-UNAM No. IN109213. F.B. acknowledges partial financial support from European Commission (FP7-ICT-2011-7) Proposal No. 288021 Network of Excellence in Internet Science and European Commission (FP7-ICT-2013-10) Proposal No. 611299 SciCafe 2.0.

### APPENDIX

The bifurcation points  $\xi_a$  and  $\xi_b$  can be found from the mean-field evolution (6) since at both values the absolute value of the derivative of this expression must be 1. For large  $k$  the mean-field approximation for the average opinion can be approximated by [7]

$$c' = \int dx \sqrt{\frac{k}{2\pi c(1-c)}} \exp\left(-\frac{k(x-c)^2}{2c(1-c)}\right) \times [\xi \tau(x; J) + (1-\xi)\tau(x; -J)]. \quad (\text{A1})$$

Expanding the right-hand-side term of this expression around  $c = 1/2$  up to first order

$$\begin{aligned} c' &= \sqrt{\frac{2k}{\pi}} \int dx \exp[-2k(x-c)^2] \\ &\quad \times [\xi \tau(x; J) + (1-\xi)\tau(x; -J)] \\ &= \sqrt{\frac{2k}{\pi}} \int dy \exp(-2ky^2) \\ &\quad \times [\xi \tau(y+c; J) + (1-\xi)\tau(y+c; -J)]. \quad (\text{A2}) \end{aligned}$$

We denote Eq. (A2) by  $g(\xi; J)$ .

To proceed we need the derivative of  $\tau$  given by Eq. (4) near  $c = 1/2$  and small  $y$ . From Eq. (4)

$$f(y; J) = \frac{\partial \tau}{\partial c} \Big|_{x=1/2+y} = \frac{4J \exp(-4Jy)}{[1 + \exp(-4Jy)]^2}.$$

We note that  $f(y; -J) = -f(y; J)$ . Then

$$g(\xi; J) = \int dy \sqrt{\frac{2k}{\pi}} \exp(-2ky^2) (2\xi - 1) f(y; J).$$

It is now straightforward to check that

$$g(1-\xi; J) = g(\xi; -J) = -g(\xi; J).$$

If  $g(\xi_a; J) = -1$  then  $g(\xi_b) = 1$  with  $\xi_b = 1 - \xi_a$  and the two bifurcation points are symmetric with respect to  $\xi = 1/2$ .

By approximating

$$f(y; J) \simeq J(1 - 4J^2y^2) \simeq J \exp(-4J^2y^2),$$

we get for  $\xi_a$

$$(2\xi_a - 1)J \sqrt{\frac{k}{2J^2 + k}} = -1,$$

i.e.,

$$\xi_a(J, k) = \frac{1}{2} \left( 1 - \frac{1}{J} \sqrt{1 + \frac{2J^2}{k}} \right).$$

The limit of this last expression when  $k \rightarrow \infty$  is  $\xi_a(J, \infty) = \frac{1}{2}(1 - 1/J)$ .

- 
- [1] C. Castellano, S. Fortunato, and V. Loreto, Statistical physics of social dynamics, *Rev. Mod. Phys.* **81**, 591 (2009).
- [2] S. Galam, *Sociophysics: A Physicist's Modeling of Psychopolitical Phenomena* (Springer, New York, 2012).
- [3] P. Nyczka and K. Sznajd-Weron, Anticonformity or independence? -Insights from statistical physics, *J. Stat. Phys.* **151**, 174 (2013).
- [4] G. Deffuant, D. Neau, F. Amblard, and G. Weisbuch, Mixing beliefs among interacting agents, *Adv. Complex Syst.* **3**, 87 (2000).
- [5] R. Hegselmann and U. Krause, Opinion dynamics and bounded confidence: Models, analysis and simulation, *J. Arti. Soci. Soc. Simul.* **5**, 1 (2002).
- [6] J. Lorenz, Continuous opinion dynamics under bounded confidence: A Survey, *Int. J. Mod. Phys. C* **18**, 1819 (2007).
- [7] F. Bagnoli and R. Rechtman, Topological bifurcations in a model society of reasonable contrarians, *Phys. Rev. E* **88**, 062914 (2013).
- [8] S. Galam, Contrarian deterministic effects on opinion dynamics: "the hung elections scenario", *Physica A* **333**, 453 (2004).
- [9] S. Galam, Modeling the forming of public opinion: An approach from sociophysics, *Global Econ. Manage. Rev.* **18**, 11 (2013).
- [10] C. Borghesi and S. Galam, Chaotic, staggered, and polarized dynamics in opinion forming: The contrarian effect, *Phys. Rev. E* **73**, 066118 (2006).
- [11] N. Masuda, Voter models with contrarian agents, *Phys. Rev. E* **88**, 052803 (2013).
- [12] N. Crokidakis, V. H. Blanco, and C. Anteneodo, Impact of contrarians and intransigents in a kinetic model of opinion dynamics, *Phys. Rev. E* **89**, 013310 (2014).
- [13] J. J. Schneider, The influence of contrarians and opportunists on the stability of a democracy in the Sznajd model, *Int. J. Mod. Phys. C* **15**, 659 (2004).
- [14] M. S. de la Lama, J. M. López, and H. S. Wio, Spontaneous emergence of contrarian-like behaviour in an opinion spreading model, *Europhys. Lett.* **72**, 851 (2005).
- [15] S. D. Yi, S. K. Baek, C.-P. Zhu, and B. J. Kim, Phase transition in a coevolving network of conformist and contrarian voters, *Phys. Rev. E* **87**, 012806 (2013).
- [16] J. Touboul, The hipster effect: When anticonformists all look the same, [arXiv:1410.8001v1](https://arxiv.org/abs/1410.8001v1).
- [17] S. E. Asch, in *Groups, Leadership and Men*, edited by H. Guetzkow (Carnegie, Pittsburgh, 1951), pp. 177-190; *Social Psychology* (Prentice Hall, Englewood Cliffs, 1952); Studies of independence and conformity: I. A minority of one against a unanimous majority, *Psychol. Monogr.* **70**, 1 (1956).
- [18] W. B. Arthur, Inductive reasoning and bounded rationality, *Am. Econ. Rev.* **84**, 406 (1994); D. Challet and Y.-C. Zhang, Emergence of cooperation and organization in an evolutionary game, *Physica A* **246**, 407 (1997); D. Challet, M. Marsili, and Y.-C. Zhang, *Minority Games* (Oxford University Press, Oxford, 2005); A. C. C. Coolen, *The Mathematical Theory of Minority Games* (Oxford University Press, Oxford, 2005).

- [19] P. S. Dodds, K. D. Harris, and C. M. Danforth, Limited Imitation Contagion on Random Networks: Chaos, Universality, and Unpredictability, *Phys. Rev. Lett.* **110**, 158701 (2013).
- [20] K. D. Harris, C. M. Danforth, and P. S. Dodds, Dynamical influence processes on networks: General theory and applications to social contagion, *Phys. Rev. E* **88**, 022816 (2013).
- [21] E. Ott, *Chaos in Dynamical Systems* (Cambridge University Press, Cambridge, 1993).
- [22] L. Boltzmann, *Vorlesungen über Gastheorie* (Barth, Leipzig, 1986), Pt. I; *ibid.* (Barth, Leipzig, 1896), Pt. II, 1898 [English translation: S. G. Brush, Lectures on Gas Theory (University of California Press, Berkeley, 1964), Chap. I, Sec. 6].
- [23] D. J. Watts and S. H. Strogatz, Collective dynamics of ‘small-world’ networks, *Nature (London)* **393**, 409 (1998).
- [24] L. Barabási and R. Albert, Emergence of scaling in random networks, *Science* **286**, 509 (1999).
- [25] M. E. J. Newman, S. H. Strogatz, and D. J. Watts, Random graphs with arbitrary degree distributions and their applications, *Phys. Rev. E* **64**, 026118 (2001).